



Contents lists available at ScienceDirect

# Remote Sensing Applications: Society and Environment

journal homepage: [www.elsevier.com/locate/rsase](http://www.elsevier.com/locate/rsase)



## Spatiotemporal analysis of atmospheric XCH<sub>4</sub> as related to fires in the Amazon biome during 2015–2020

Luciano de Souza Maria <sup>a,\*</sup>, Fernando Saragosa Rossi <sup>a</sup>, Luis Miguel da Costa <sup>a</sup>, Marcelo Odorizzi Campos <sup>a</sup>, Juan Carlos Guerra Blas <sup>a</sup>, Alan Rodrigo Panosso <sup>a</sup>, Joao Lucas Della Silva <sup>b</sup>, Carlos Antonio da Silva Junior <sup>b</sup>, Newton La Scala Jr <sup>a</sup>

<sup>a</sup> São Paulo State University (Unesp), Jaboticabal, 14884-900, Brazil

<sup>b</sup> University of the State of Mato Grosso, Sinop, 78580-000, Brazil

### ARTICLE INFO

#### Keywords:

Arc of deforestation  
Climate changes  
Fire foci  
Seasonality  
Soil moisture  
 $\text{XCO}_2$

### ABSTRACT

Studies that focus on the concentration of methane and its relationship with fires in the Amazon have become relevant in the current scenario, especially due to the increasing environmental degradation associated with climate change. Therefore, the main objective of the study was to investigate the spatial-temporal variability in the observations of XCH<sub>4</sub> in the time series of 2015 a 2020 and understand the correlations between XCH<sub>4</sub> and the fire foci number, CO<sub>2</sub> anomalies and biophysical variables (temperature and soil moisture) under the Amazon biome. For number of active fires foci (Fire Foci) and Land Surface Temperature (LST) were obtained through the Moderate Resolution Imaging Spectroradiometer (MODIS) sensor, and the atmospheric concentrations of the averaged column of methane (XCH<sub>4</sub>) and carbon dioxide (XCO<sub>2</sub>) were obtained by the Greenhouse gases Observing SATellite (GOSAT) satellites and Orbiting Carbon Observatory-2 (OCO-2), respectively. The Soil Moisture (SMAP) was obtained through satellite Soil Moisture Active Passive (SMAP). The analysis was carried out in the dry and wet seasons, and the XCH<sub>4</sub> presented an annual mean and standard error of  $1794 \pm 5.3$  ppb for the rainy season, while for the dry period, the XCH<sub>4</sub> was  $1789 \pm 5.6$  ppb. For the spatial distribution of XCH<sub>4</sub>, a significant correlation ( $r = 0.53$  and  $p < 0.05$ ) was observed between XCH<sub>4</sub> and Anomaly XCO<sub>2</sub> in the dry season, possibly justified by the increase in fire foci. Additionally, in the dry period, XCH<sub>4</sub> was significantly correlated with SMAP ( $r = 0.97$ ,  $p < 0.01$ ), validating the hypothesis of a strong relationship between the variables. The temporal variability of XCH<sub>4</sub> was significant for SMAP ( $r = 0.65$  and  $p < 0.01$ ), similar to the significance of the LST variable ( $r = 0.66$  and  $p < 0.01$ ). Thus, the temporal distribution of XCH<sub>4</sub> was positively related to both soil moisture and land surface temperature. Therefore, considering more frequent droughts and the predominance of fires in the region, as well as the increase in global average temperature, there will be an increase in greenhouse gas (GHG) emissions, especially methane, further impacting the Amazonian ecosystem, which is already vulnerable to climate change.

### 1. Introduction

The Brazilian Amazon biome has a high environmental representation due to its great biodiversity of plants and animals and is therefore considered the largest continuous tropical forest on Earth, occupying 3% of the terrestrial territory (Heinrich et al., 2021).

\* Corresponding author.

E-mail address: [luciano.maría@unesp.br](mailto:luciano.maría@unesp.br) (L. de Souza Maria).

Stands out especially for its capacity as a carbon sink (C) and consequent mitigation of the greenhouse effect (Antonelli et al., 2018; Brienen et al., 2015; Heinrich et al., 2021).

However, there is a high vulnerability of this biome due to changes in land use and climate (Marengo et al., 2018; Nobre et al., 2016), mainly in areas where forests are most degraded (Saatchi et al., 2021), which are threatened by deforestation and fire (da Silva Junior et al., 2022; Eufemia et al., 2022; Le Roux et al., 2022; Teodoro et al., 2022; Eufemia et al. (2022); Le Roux et al. (2022); Teodoro et al. (2022)) and the consequent increase in the emission of greenhouse gases (GHG) into the atmosphere (Aragão et al., 2018; Da Silva Junior et al., 2020). In addition, this environment has been affected by increasingly frequent and extreme droughts, which tend to negatively modify the equilibrium state of humid tropical forests in the coming decades (Anderson et al., 2018; Nobre et al., 2016; Silva et al., 2018).

According to the Intergovernmental Panel on Climate Change (IPCC) report (Intergovernmental Panel on Climate Change - IPCC et al., 2022), current atmospheric GHG levels expose the human inability to reduce their impact on the climate. Currently, the atmospheric concentration of methane ( $\text{CH}_4$ ) has reached 1877.3 ( $\pm 3.3$ ) ppb (Intergovernmental Panel on Climate Change - IPCC et al., 2022), an increment of 2.6 times greater than the concentrations prior to the preindustrial revolution period (Nisbet et al., 2019; Saunois et al., 2020). In addition to alarming atmospheric levels, methane has a heating potential 28 times greater (100 years) than  $\text{CO}_2$  (Intergovernmental Panel on Climate Change - IPCC et al., 2022). According to the sixth assessment report (AR6) of the IPCC, despite the shorter length of stay (~10 years), methane contributed approximately 16% (0.54  $\text{Wm}^{-2}$ ) of the total effective radiative forcing (ERF) among the GHGs for the period 1750–2019.

Regarding the emission sources, wetlands stood out among the interannual variability of  $\text{CH}_4$  sources (Bousquet et al., 2006) and, to a lesser extent, emissions from incomplete combustion of biomass and soil carbon during foci of forest fires (Kirschke et al., 2013). The frequency and severity of droughts increase the occurrence of fire foci (Anderson et al., 2018; Basso et al., 2021; Morgan et al., 2019), which consequently increase  $\text{CH}_4$  emissions, especially in areas with large amounts of biomass, mainly in the tropics, where tropical forests (Amazon Forest) are burned (Saunois et al., 2020), and emit high amounts of  $\text{CH}_4$  into the atmosphere due to incomplete burning of forest biomass (Basso et al., 2021).

The GOSAT mission aimed to assess the sources and sinks of GHGs to estimate atmospheric concentrations of  $\text{CH}_4$  ( $\text{XCH}_4$ ) at regional and global scales. Therefore, it sought to contribute to the generation of information and better management of environmental resources, in addition to assisting research aimed at understanding the global ecosystem carbon cycle, through the observation of the averaged atmospheric column  $\text{CO}_2$  ( $\text{XCO}_2$ ) (Guo et al., 2017; Oguma et al., 2011).

Similarly, the OCO-2 mission launched in July 2014 by NASA also makes it possible to observe  $\text{XCO}_2$  from space (Frankenberg et al., 2015). Thus,  $\text{CO}_2$  emissions from forest fires have been contemplated by several studies, whether in boreal forests (Guo et al., 2017, 2019) or rainforests (Heymann et al., 2017; Jiang et al., 2021; Yin et al., 2018). However, it is worth noting that fires in tropical forests tend to produce more carbon monoxide (CO) and  $\text{CH}_4$  per unit of fuel burned (Webb et al., 2016; Wecht et al., 2014; Wilson et al., 2020). The frequency and severity of droughts accentuate the occurrence of fires, which consequently increase  $\text{CH}_4$  emissions (Anderson et al., 2018; Basso et al., 2021; Morgan et al., 2019).

Despite the importance of the topic, there are several gaps in the understanding of the temporal distribution and spatialization of fires and their relationship with  $\text{CH}_4$  emissions, especially for those occurring in the Amazon biome. Geostatistical interpolation methods, such as kriging, are important ways to relate the distribution of  $\text{XCH}_4$  in space and over the years of study (Li et al., 2022). This method has been used to fill important gaps in regard to GHG, especially in the period of greater occurrence of fires and when comparing dry and wet periods (Devkota, 2021; Falahatkar et al., 2017; Li et al., 2022).

Demonstrating the advances and opportunities around the subject, this study sought to use two main hypotheses: (i) the spatialization of  $\text{XCH}_4$  seasonality is related to fire foci and (ii) there is a relationship between  $\text{XCH}_4$  and soil moisture for the dry and wet periods under the Amazon. Thus, the objective of the study was to investigate the patterns of temporal and spatial variability of the atmospheric concentration of  $\text{XCH}_4$  and the relationships with the Moderate Resolution Imaging Spectroradiometer (MODIS) products (Fire Foci and Land Surface Temperature - LST),  $\text{XCO}_2$  anomalies and the product of Soil Moisture Active Passive (soil moisture) in the Brazilian Amazon.

## 2. Material and methods

### 2.1. Study area

The study area comprises the Brazilian Amazon Forest biome (Fig. 1), with a territorial extension of 6 million  $\text{km}^2$ , covering the states of Acre, Amapá, Amazonas, Pará, Roraima, Rondônia and partially the state of Maranhão, Mato Grosso and Tocantins (IBGE, 2020).

According to the Köppen climate classification, the predominance of climate classes Am (monsoons) and Aw (with dry winters) occurs under the study area. The annual precipitation varies from 1800 to 3000 mm, and the average temperature is 26.8 °C in the Amazon region (Alvares et al., 2013). The dry period is evidenced from May to October, and the rainy season extends from November to April each year (Zemp et al., 2017).

### 2.2. Land surface temperature data

In Land Surface Temperature (LST) analysis, daytime and nighttime data from the product MOD11A2 V006 were used (Wan, 2008) produced and provided by NASA (National Aeronautics and Space Administration) from the MODIS sensor with 8 days with a spatial resolution of 1  $\text{km}^2$ , in which images with fewer invalid pixels were chosen.

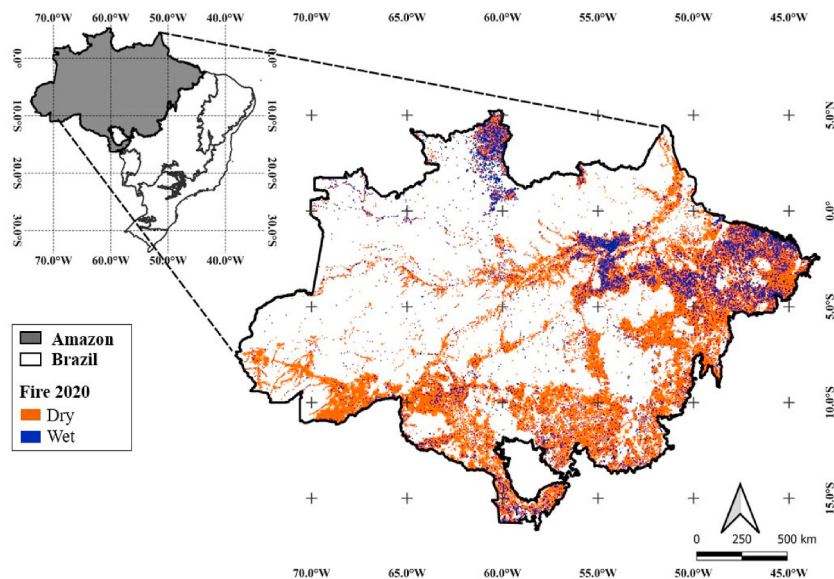


**Fig. 1.** The study area is located in the Brazilian Amazon Forest Biome with fire foci from 2020 obtained from Moderate Resolution Imaging Spectroradiometer (MODIS) data using swath products (MOD14/MYD14) (Gigli et al., 2003).

The annual average of the MOD11A2 product data was calculated using the Raster Calculator tool of the QGIS 3.16.4-Hannover software. Posteriorly, the results of calculating the surface temperature without units were multiplied by a scale factor of 0.02 to obtain Kelvin (K) degrees, then converted to Celsius ( $^{\circ}\text{C}$ ) (Equation (1)) and divided by 8 to obtain daily values (Wan, 2008).

$$\text{LST\_Celsius\_Day} = \frac{(LST_{\text{Day}} \text{ km} * 0.02) - 273.25}{8} \quad (1)$$

### 2.3. Fire focus data

The daily data of fire foci of the time series were obtained between 2015 and 2020. Data were obtained directly from the Atmosphere Near real-time Capability for EOS (LANCE) Fire Information for Resource Management System (FIRMS) (<https://firms.modaps.eosdis.nasa.gov/>), calculated through the product obtained by the MODIS sensor onboard the TERRA/AQUA satellites. Posteriorly, for data processing, the daily averages of the daily observations of Count Fire foci were calculated for each pixel (1 km). Then, the number of points (n) of fire foci greater than 8 in each pixel was considered. It is worth mentioning that the amount of n influences the construction of better estimates of the parameters of fires.

### 2.4. Orbiting Carbon Observatory 2 (OCO-2) data

The Orbiting Carbon Observatory-2 (OCO-2) satellite was launched by NASA in July 2014 and has made the atmospheric concentration of carbon dioxide ( $\text{CO}_2$ ) available as a primary product since September 2014 (Crisp et al., 2017). According to Crowell et al. (2019), this tool made it possible to estimate  $\text{CO}_2$  sinks and sources on regional scales. The average concentration of  $\text{CO}_2$  in a column of dry air ( $\text{XCO}_2$ ) extends from the Earth's surface to the top of the atmosphere, approximately 740 km (Crisp et al., 2012; O'Dell et al., 2012).

The data are made available by the OCO-2 (NASA) platform: [https://oco2.gesdisc.eosdis.nasa.gov/data/OCO2\\_DATA/](https://oco2.gesdisc.eosdis.nasa.gov/data/OCO2_DATA/). The  $\text{XCO}_2$  values (version V9r) are retrieved using the algorithm of O'Dell et al. (2012); therefore, OCO-2 enables products to have a spatial resolution of  $2.25 \times 1.29$  km and a temporal resolution of 16 days. Furthermore, the observations that have the best visibility and the lowest level of uncertainty were considered (quality flag = 0 and alert level < 12) (Nikitenko et al., 2020; Rossi et al., 2022).

Therefore, the increase in  $\text{XCO}_2$  for the time series studied (2015–2020) was corrected based on  $\text{XCO}_2$  observations for the entire Brazilian territory, due to the greater number of data collection points, as well as the low number of points in the sample area in the Amazon biome. Thus, this work characterizes the concentration of  $\text{CO}_2$ , as well as the relationships between the number of fire foci to dry and humid periods.

### 2.5. Anomaly $\text{XCO}_2$

Due to the long lifetime of  $\text{CO}_2$  in the atmosphere, the high difficulty of extracting information from the spatial distributions of the emission areas from  $\text{XCO}_2$  satellite measurements, with the averages for each year, becomes evident. Thus, the accumulation of  $\text{CO}_2$  in the atmosphere demonstrates a growth rate of approximately 2–3 ppm per year (Hakkainen et al., 2016). It currently has a general background level of approximately  $418 \pm 0.2$  ppm.

Therefore, to extract the information from the anthropogenic signatures of orbital recoveries (OCO-2), the  $\text{XCO}_2$  concept was used (Hakkainen et al., 2016). In the present study, the difference between the individual value of  $\text{XCO}_2$  observed by the OCO-2 and the background (the daily median of  $\text{XCO}_2$  over an area of Brazilian territory) was calculated according to equation (2).

$$\text{XCO}_2 \text{ (anomaly)} = \text{XCO}_2 \text{ (individual)} - \text{XCO}_2 \text{ (daily median from Brazil)} \quad (2)$$

## 2.6. XCH<sub>4</sub> data from the GOSAT satellite

The GOSAT (The Greenhouse gases Observing SATellite) satellite stands out for two main onboard sensors: the Thermal and Near Infrared Sensor for Carbon Observations - Fourier Transform Spectrometer (TANSO-FTS) and the Cloud and Aerosol Imager (TANSO-CAI). It is worth noting that TANSO-FTS has four bands, one related to the TIR (5500–14300 nm), used in the description of the vertical profile of the CO<sub>2</sub> concentration in the upper troposphere and another three for Short-Wave Infrared (SWIR) in the spectral range of 760, 1600 and 2000 nm, used in estimating the average CO<sub>2</sub> column concentrations (XCO<sub>2</sub>). The images generated through the TANSO-CAI sensors occur in four bands (380, 675, 870 and 1600 nm) capable of offering spatial resolutions of 500 m, beyond assisting applications in mapping clouds and atmospheric aerosols (Guerlet et al., 2013; Ross et al., 2013).

GOSAT allows a revisit at the same location in periods of 3 days (temporal resolution) and was developed in order to characterize emission sources and sinks on a continental scale, having a spatial scale cover of approximately 10 km, in circular pixels separated by about 270 km (Parker et al., 2015). Total methane column data were obtained from the University of Leicester GOSAT Proxy with version 9.0. The data are public, available at [https://data.ceda.ac.uk/neodc/gosat/data/ch4/nceov1.0/CH4\\_GOS\\_OCPR/](https://data.ceda.ac.uk/neodc/gosat/data/ch4/nceov1.0/CH4_GOS_OCPR/) (Parker et al., 2015). The average dry air column methane molar fractions (XCH<sub>4</sub>) were derived using the proxy method from CO<sub>2</sub> emission models (Parker et al., 2011, 2015). Thus, the method multiplies the ratio XCH<sub>4</sub>/XCO<sub>2</sub> by a model of in situ observations XCH<sub>4</sub>, considering the average of each year (Parker et al., 2011, 2015).

The XCO<sub>2</sub> models were based on local measurements of land surfaces using the median metric from the global models GEOS-Chem (Feng et al., 2011), Carbon Tracker (Peters et al., 2007) and LMDZ (Chevallier et al., 2010). It is worth noting that the GOSAT Proxy product was validated through measurements on aircraft in the Amazon region (Tunnicliffe et al., 2020; Wilson et al., 2020).

## 2.7. Soil Moisture Active Passive (SMAP) data

NASA's mission for the Soil Moisture Active Passive (SMAP) satellite enables observations of soil moisture in orbit. The SMAP carries L-band radiometry instruments capable of measuring the surface brightness temperature, thus providing the dimensioning of soil surface moisture with a resolution of approximately 5 cm from the soil (Cui et al., 2018; Hyoung, 2021).

The equipment has a spatial resolution of approximately 9 km and a daily temporal resolution (Entekhabi et al., 2010). To enable the desired relationships and analysis, monthly averages were used for the time series from 2015 to 2020. Therefore, the data were obtained through R software (R Development Core Team, 2022) using the "rgee" package (Aybar et al., 2020).

## 2.8. Digital processing

For understand the natural and regional variability of XCH<sub>4</sub> and their relationship to biophysical variables were used the regression method to subtracted the background of the XCH<sub>4</sub> to remove the trend from data. Using the coordinates obtained on the GOSAT platform (JAXA) with pix of 10.5 km (0.1° × 0.1°), it established a pattern to attenuate the difference between the spatial and temporal resolutions and the different orbital sensors. Corroborating studies similar to the present study, using satellites with different resolutions (da Costa et al., 2022a; Falahatkar et al., 2017).

## 2.9. Temporal statistical analysis

To study the temporal variation of the variables, with monthly distribution graphs were constructed for XCH<sub>4</sub> GOSAT, LST, SMAP and anomaly XCO<sub>2</sub> data associated with the Amazon biome in the time series (2015–2020). Subsequently, Pearson's correlation (*r*) was performed with the annual means of the variables over the time series. Finally, the histograms were generated with the number of fires and the anomalous atmospheric concentrations of the average column of carbon dioxide (XCO<sub>2</sub>) to observe the relationships between variables.

## 2.10. Grey relation analysis

Grey Relation analysis (GRA) consists of a quantitative analysis technique to measure the similarity between variables, it makes it possible to evaluate the correlation between variables by relational degree (Deng, 1982). To show the correlation between the mean value of the three variables (Fire foci, SMAP and anomaly XCO<sub>2</sub>) and the mean value of XCH<sub>4</sub> GOSAT for the dry and wet season in 2015–2020, the grey relational analysis makes it possible to understand the relationships between the variables. For this we calculate the correlation coefficient by Equation (3).

$$\xi_i(k) = \frac{\min_{i} \max_{k} |t(k) - X_i(k)|}{\max_{i} \min_{k} |t(k) - X_i(k)|} \quad (3)$$

Where:  $\xi_i(k)$  is the grey relational coefficient of  $X_i$  to  $t$  at time  $k$ , and  $\xi$  is the resolution coefficient (generally between 0 and 1, 0.5 in this study), where  $\min_{i} \max_{k} |t(k) - X_i(k)|$ .

and  $\max_{i} \min_{k} |t(k) - X_i(k)|$  are the two-level minimum and two-level maximum, respectively.

### 2.11. Geostatistical analysis

The XCH<sub>4</sub> (GOSAT) time series data between 2015 and 2020 were subjected to experimental variogram analysis (Webster and Oliver, 1990) and then ordinary kriging for the estimation of the variable in unsampled locations. The sampling grid was determined in grids spaced between 0.5° and 3-day intervals for the entire historical series. Thus, the entire Brazilian territory was considered due to the greater number of data collection points, as well as the low number of points in the sample area in the Amazon biome.

The data used came from two periods: the first for the humid period (Wet), delimited for the months of November, December, January, February, March and April; and the second for the dry period (Dry), delimited for the months of May, June, July, August, September and October. Therefore, it was possible to establish patterns of spatial variability of XCH<sub>4</sub> for the two periods studied and then estimate the semivariance at a given distance. The semivariance was estimated by equation (4):

$$\hat{\gamma}(h) = \frac{1}{2N(h)} \times \sum_{i=1}^{N(h)} [Z(x_i) - Z(x_i + h)]^2 \quad (4)$$

where  $h$  is the distance between pairs of points;  $N(h)$  is the number of pairs of points separated by distance  $h$ ;  $Z(x_i)$  is the value of XCH<sub>4</sub> at point  $x_i$ ; and  $Z(x_i + h)$  is the value of XCH<sub>4</sub> at point  $x_i + h$ .

To determine the model that best fit the experimental variogram, the cross-validation technique was used. This technique consists of removing each observation belonging to the data set and estimating the value by the interpolation method (ordinary kriging). Thus, the model becomes more capable of estimating the observed values. According to Isaaks and Srivastava (1989), the use of the linear regression equation between predicted and observed values will depend on the estimated values closest to the bisector – intercept equal to zero and slope equal to unity. Therefore, to better expose the theoretical models used, these were demonstrated in equation (5) (Spherical Model) and 6 (Gaussian Model):

$$\hat{\gamma}(h) = C_0 + C_1 \left[ \frac{3}{2} \left( \frac{h}{a} \right) - \frac{1}{2} \left( \frac{h}{a} \right)^3 \right] \quad (5)$$

where  $0 < h < d$ ,  $\hat{\gamma}(h) = C_0 + C_1$ , and  $h > a$ .

$$\hat{\gamma}(h) = C_0 + C_1 \left\{ 1 - \exp \left[ -3 \left( \frac{h}{a^2} \right) \right] \right\} \quad (6)$$

where  $0 < h < d$ , and  $d$  is the maximum distance at which the variogram was defined. The nugget ( $C_0$ ), sill ( $C_0 + C_1$ ), and range ( $a$ ) are important parameters for the variogram.

The ratio between Nugget and sill makes it possible to infer as an indicator to classify the spatial dependence of the data set (Cambardella et al., 1994). Therefore, a ratio greater than 0.75 provides a high spatial dependence of the data.

The parameters of the fitted models (Spherical and Gaussian) for the experimental variograms made it possible to estimate XCH<sub>4</sub> values in unsampled locations in the Amazon biome. In the elaboration of maps with the spatial patterns of methane for the wet and dry periods, the ordinary kriging technique was used, described by equation (7):

$$Z^*(x_o) = \sum_{i=1}^N \lambda_i Z(x_i) \quad (7)$$

where  $Z^*$  is the value to be estimated for the unsampled data of  $x_o$ , the number of measured values  $Z(x_i)$  involved in the estimate and  $i$  is the weights associated with the measured value of  $Z(x_i)$ .

For the descriptive statistics, with the calculation of the semivariance and the appropriate adjustments of the models, was used the software R.

After adjusting the models, the estimated values in unsampled areas in the Amazon biome were determined by the ordinary kriging interpolation method (Isaaks and Srivastava, 1989; Trangmar et al., 1986). For the elaboration of the spatial maps of the wet and dry periods, we used the QGIS software.

For the wet period of the 2015 and 2018 time series, the IDW methods were used, justified by the nugget and sill values being equal to 3.34 (2015) and 5.55 (2018); therefore, there is no spatial dependence through the experimental variogram; however, this approach was also used for the spatialization of GHGs in recent studies (da Costa et al., 2022b). The description of the model used is shown in equation (8):

$$Z_j = \frac{\sum_{i=1}^n \frac{Z_i}{h_{ij}\beta}}{\sum_{i=1}^n \frac{1}{h_{ij}\beta}} \quad (8)$$

where  $Z_j$  = estimated value for location  $j$ ;  $Z_i$  = sample value measured for sample  $i$ ;  $h_{ij}$   $\beta$  = distance between  $Z_j$  and  $Z_i$ ; and  $\beta$  = weighting power.

### 3. Results

#### 3.1. Temporal

In the XCH<sub>4</sub> time series, it was observed that for the dry period (May to October), the lowest values were recorded (close to 1765 ppb), while the highest values (1809 ppb) were observed in the wet period (November to April) (Fig. 2). Similarly, the highest values of XCH<sub>4</sub> with an increase in amplitude were observed in the wet period, as well as increases in SMAP and LST (Fig. 2). Based on our results, noted a lagging effect of SMAP and LST, mainly in the period of 2015 and 2016, this period there was a phase strong of the ENSO (El Niño-Southern Oscillation) in the Amazon region. However, between XCH<sub>4</sub> and Anomaly, XCO<sub>2</sub> presented an inverse amplitude with peak observations in January and February for XCH<sub>4</sub>, and for Anomaly, variable XCO<sub>2</sub> peaks were observed in July and August (Fig. S3).

Pearson's correlation coefficient of XCH<sub>4</sub> GOSAT by temporal distribution between SMAP and LST variables was an intermediate positive correlation for the monthly means ( $p < 0.05$ ). On the other hand, we observed a significant ( $p < 0.05$ ) negative intermediate strength between XCH<sub>4</sub> GOSAT and XCO<sub>2</sub> Anomaly ( $r = -0.648$ ). The XCO<sub>2</sub> anomaly also relates negatively to LST ( $r = -0.66$ ) and SMAP ( $r = -0.59$ ) (Fig. 3).

Fig. 4 illustrates the average daily anomaly obtained by OCO-2 from 2015 to 2020. It is worth noting that the largest XCO<sub>2</sub> anomalies were observed for 2018. Highlighting 2019 and 2020, there were 388,288 fire foci throughout Brazilian territory, espe-

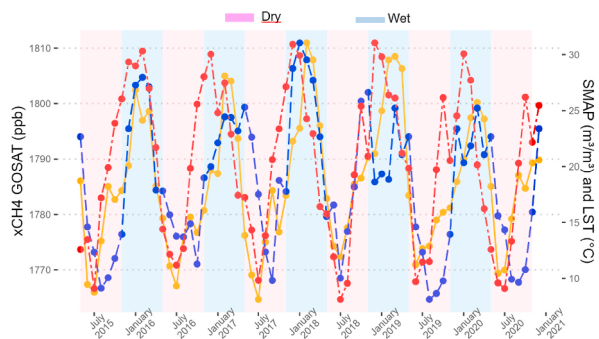


**Fig. 2.** Time series of XCH<sub>4</sub> GOSAT (orange line and solid), Soil Moisture Active Passive (SMAP; blue line and long dash) and Land Surface Temperature (LST; red line and twodash) of monthly averages over the Amazon biome. Units for XCH<sub>4</sub> GOSAT, SMAP and LST are ppb,  $\text{m}^3 \text{m}^{-3}$  and  $^{\circ}\text{C}$ . Pink area is to dry period and blue area is to wet period. (For interpretation of the references to colour in this figure legend, the reader is referred to the Web version of this article.)

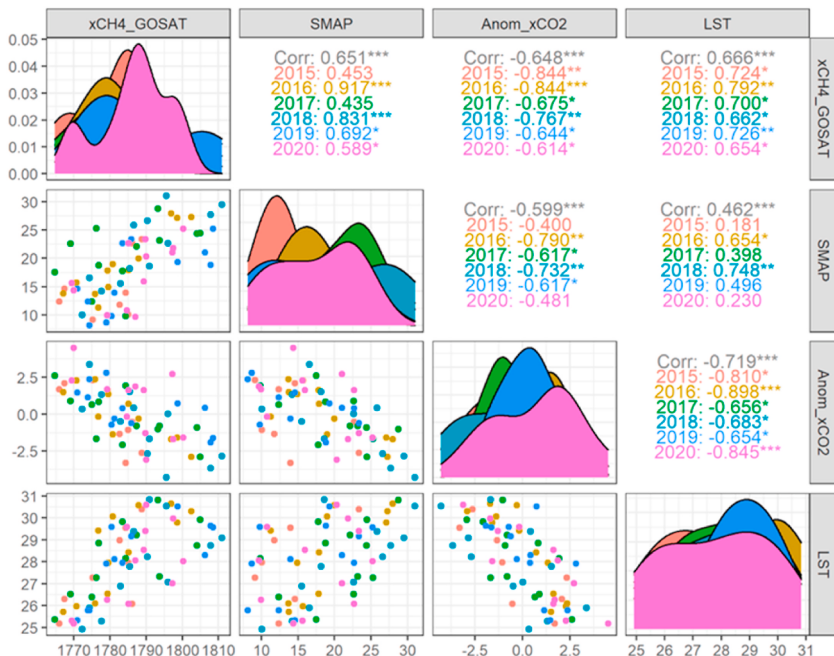


**Fig. 3.** Heatmap of Pearson's temporal correlation matrix for the studied variables XCH<sub>4</sub> GOSAT, Anom (Anomaly XCO<sub>2</sub>), Fire Foci, Land Surface Temperature (LST) and Soil Moisture Active Passive (SMAP).

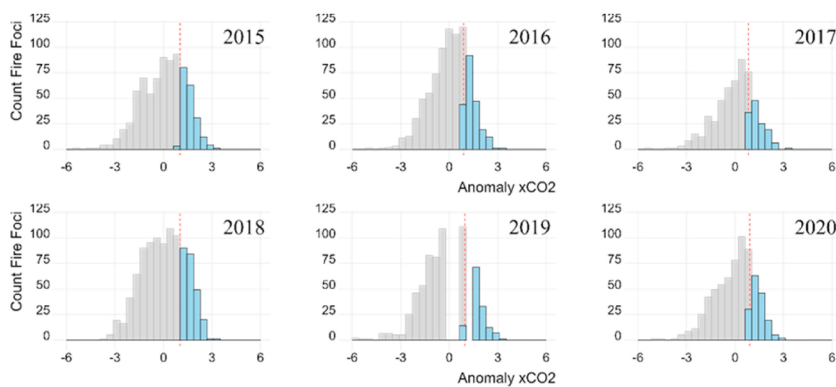


**Fig. 4.** Histograms of the relationships between the number of fires and the anomalous atmospheric concentrations of the average column of carbon dioxide (XCO<sub>2</sub>), highlighted in blue histograms. (For interpretation of the references to colour in this figure legend, the reader is referred to the Web version of this article.)

cially on the Amazon biome, with 49.5% (192,337) of fire foci for the 2019–2020 biennium (Fig. 4) (INPE - Instituto Nacional de Pesquisas Espaciais, 2021).

### 3.2. Spatial

For the analysis of the spatial variability of XCH<sub>4</sub> GOSAT, the parameters of the experimental semivariograms were initially established (Table 1). For the wet season, in relation to the degree of spatial dependence (GSD), in 2015 and 2018 (nugget = sill), there was no spatial dependence. However, for 2020 (<0.25), there was also a strong spatial dependence for the wet season. For the dry period, all years presented moderate GSD (0.25–0.75).

The spherical and Gaussian models showed good fits for the experimental semivariograms for the XCH<sub>4</sub> variable (Table 1), and they described spatial patterns in the dry and wet periods in the areas inserted in the Amazon biome. Thus, it is worth noting that the Gaussian models allowed the use in regular and continuous phenomena, while the spherical models explained the variables with high continuity, or less erratic in small distances (Isaaks and Srivastava, 1989).

The Grey Relational Correlation Coefficient were developed to understand the similarity between the variables in the spatial distribution (Fig. S4). In general, it can be observed that most of the correlations between the variables with range from 0.73 to 0.81. The count of Fire foci showed low similarity ( $p < 0.75$ ) with the variable XCH<sub>4</sub> for the dry period (XCH<sub>4</sub> Wet). For the other variables the grey correlation coefficients of the other indexes are higher than 0.75, which are at a relatively high level. (Fig. S4).

The maps of the spatial patterns of XCH<sub>4</sub> in the dry period showed, for 2015, 2016, 2018 and 2019, the largest observations in the southeastern portion of the Amazon biome (Fig. 5). However, for 2017, it was found that the central Amazon region had the highest observations, and for 2020, there was no pattern, possibly due to a lower number of observation points (<450).

In Fig. 6, it was observed that the SMAP ( $m^3 m^{-3}$ ) presented the highest observations in the northwest portion, justified by the highest average annual rainfall for the region. However, our results point which southeast and northeast portions, the lowest humidity values were observed for areas inserted in the Amazon biome in the analyzed time series (2015–2020) (Figs. 5 and 6).

For the wet period, there was no pattern in the spatialization of XCH<sub>4</sub> for the Amazon biome (Fig. 7). The period of high precipitation for the entire Amazon region, with high cloudiness, reduces the number of significant points for the period. It is also worth noting

**Table 1**

Models and semivariogram parameters for XCH<sub>4</sub> GOSAT in wet and dry periods for 2015–2020 in areas in the Amazon biome.

Year	Model	Nugget	Sill	A(m)	SRS	SDD
<b>Wet</b>						
2015	–	3.34	3.34	0.00	–	–
2016	Gau	9.55	23.68	25.73	225.20	0.40
2017	Sph	3.73	7.72	13.50	32.32	0.48
2018	–	5.55	5.55	0.00	–	–
2019	Gau	6.65	8.50	12.03	82.47	0.78
2020	Sph	0.03	84.74	13.48	500.35	<0.01
<b>Dry</b>						
2015	Sph	6.17	11.16	13.52	367.43	0.55
2016	Gau	7.71	13.37	13.80	223.88	0.57
2017	Gau	9.00	15.00	20.78	684.25	0.60
2018	Sph	7.73	14.36	20.68	1755.05	0.54
2019	Sph	8.00	15.00	16.00	1899.23	0.53
2020	Sph	5.66	8.61	2.33	87.49	0.66

SDD Spatial dependence degree = Nugget/Sill, Strong for values lower than 0.25; moderate for values between 0.25 and 0.75; weak for values higher than 0.75 (Cambardella et al., 1994); SRS sum of residue squares; Sph spherical; Gau Gaussian.

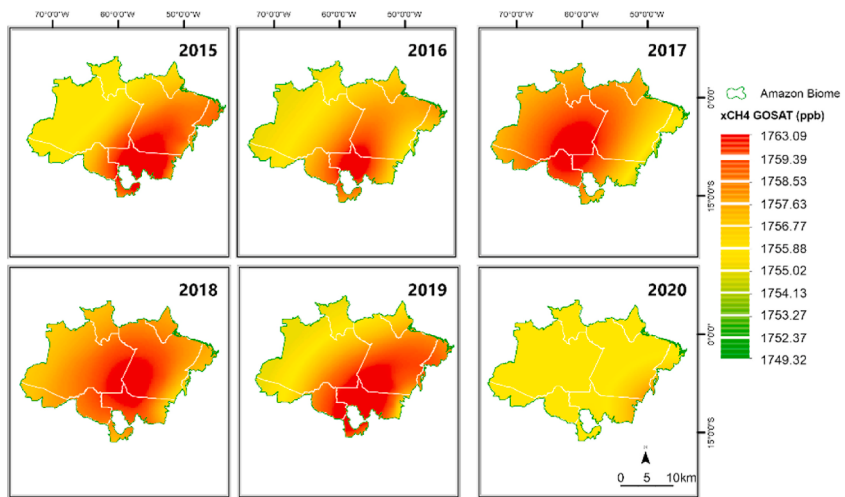


**Fig. 5.** Maps of XCH<sub>4</sub> for dry period in the Amazon biome from the period of 2015–2020 applying kriging methodology.

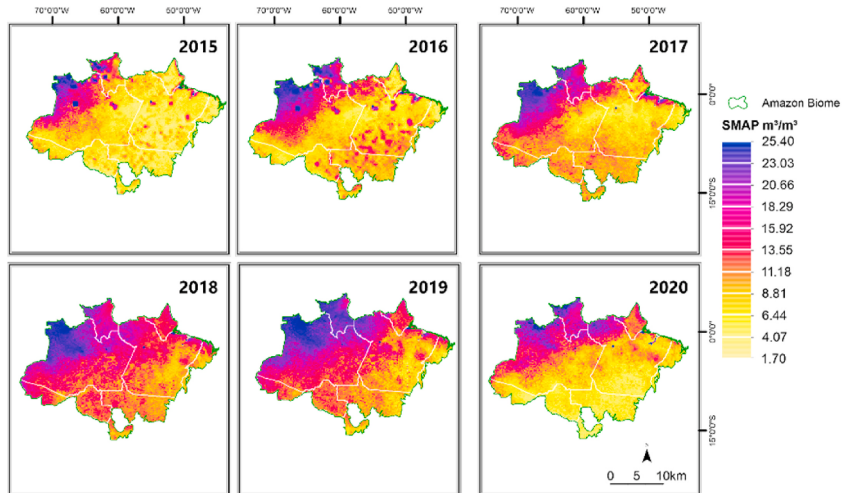


**Fig. 6.** Maps of Soil Moisture Active Passive – SMAP ( $\text{m}^3 \text{ m}^{-3}$ ) from dry period to 2015–2020 in the Amazon biome.

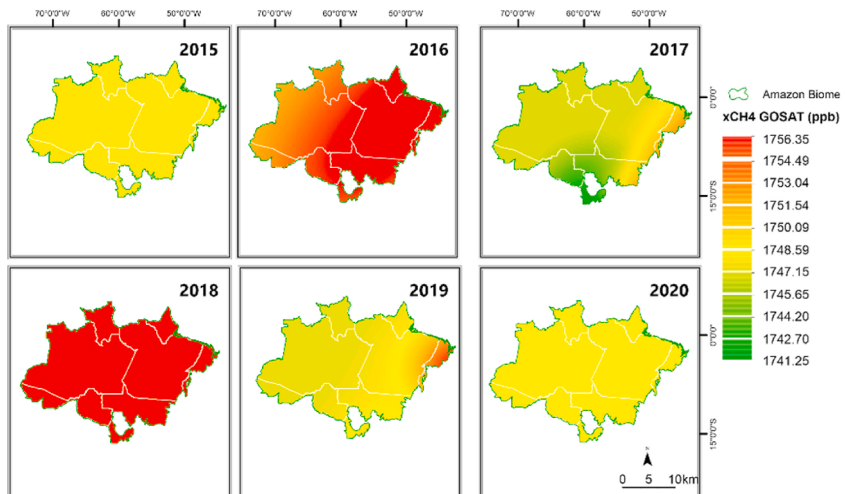


**Fig. 7.** Maps of XCH<sub>4</sub> for wet period in the Amazon biome from the period of 2015–2020 applying kriging methodology.

that the period provides the greatest uncertainties in orbital observations for greenhouse gas monitoring satellites, especially for methane.

The distribution of soil moisture for the wet season was consistent with the spatial distribution of XCH<sub>4</sub>, especially for 2016 (Fig. 8). The northern portion of the Amazon biome also had lower soil moisture for 2016, differing from the other years analyzed in the time series.

#### 4. Discussion

In the temporal distribution of XCH<sub>4</sub>, it was understood that the peak in the rainy season (January and February) provides the highest values observed in the time series. Thus, it is important to highlight that SMAP and LST were positively correlated with the atmospheric concentration of XCH<sub>4</sub> in the Amazon biome. Thus, it corroborated validating hypothesis "ii" of the strong relationship between the XCH<sub>4</sub> and SMAP variables. It is also worth noting that the amplitudes of XCH<sub>4</sub> and Anomaly XCO<sub>2</sub> have peak amplitudes of different periods. However, in the rainy season, the highest concentrations of XCH<sub>4</sub> were observed, and lower concentrations of XCO<sub>2</sub> were also observed. The low values of CO<sub>2</sub> anomalies are explained by the greater photosynthetic activity of plants and the greater availability of water in the rainy season (Albright et al., 2022). Likewise, this justifies the higher amplitudes with peaks in July and August, coinciding with higher occurrences of fires (Carvalho et al., 2021; Pontes-Lopes et al., 2021).

Another highlight is that the variability of XCO<sub>2</sub> concentration can be driven by the increase in fire foci (Detmers et al., 2015). Hence, a relationship between the increase in Anomaly XCO<sub>2</sub> and fire foci was observed (Fig. 4). Thus, it was also observed that the spatial distribution of XCH<sub>4</sub> and the Anomaly XCO<sub>2</sub> for the dry period showed a moderate similarly between the variables, corroborated by Grey Relational Correlation Coefficient (Fig. S4), possibly justified by the occurrence of fire foci in the period.

Otherwise, there was a significant positive correlation ( $r = 0.97$ ,  $p < 0.05$ ) between XCH<sub>4</sub> and SMAP for the dry period for the spatial distribution of XCH<sub>4</sub>. Thus, as for the temporal distribution, the spatial distribution also validated hypothesis "ii" about a strong relationship between the variables. Therefore, a pattern of spatial distribution of the variable XCH<sub>4</sub> was observed for the dry period that matches the pattern of spatialization of the SMAP, except for 2020.

The southeastern and northwestern portions of the Amazonian territory had the highest XCH<sub>4</sub> hotspots (Fig. 5). This result is explained by the agricultural activity in the region and mainly by the intense burning of local biomass (Wilson et al., 2020). According to Wilson et al. (2020), the region is known as the "arc of Amazon deforestation", characterized by the intense conversion of forests into pastures and agricultural crops in recent decades.

Crippa et al. (2021) highlight that the methane emissions for Brazil from biomass burning were 1.4 Tg between 2015 and 2018. The MapBiomas (2022) platform showed that 31 million hectares were burned between 2015 and 2020 in the Amazon biome, occurring mainly in the "arc of deforestation". During this period, the fires were concentrated in the months of August, September and October (INPE - Instituto Nacional de Pesquisas Espaciais, 2021). This period falls within the final dry months, when the vegetation is under stress conditions due to lack of rain (Alvares et al., 2013; Zemp et al., 2017).

The impact of fire foci on XCH<sub>4</sub> Wet was significant in Pearson's correlation analysis ( $p < 0.05$ ), demonstrating that the action of fire contributed positively to higher atmospheric concentrations of XCH<sub>4</sub> in the wet season (Fig. S3). On the other hand, XCH<sub>4</sub> Dry did not correlate with fire foci. According Andersen et al. (1998), nonflooded forest soils become sources of CH<sub>4</sub> when devoid of vegetation, especially in the wet season.

The exposure of forest soil caused by the burning of aerial biomass favors solar incidence, consequently impacting the temperature and humidity of the soil, especially close to the surface (Acero and González-Asensio, 2018). As described for MapBiomas (2022), the period of intense fires occurs mostly at the end of the dry season in the Amazon region; therefore, the beginning of the wet season oc-

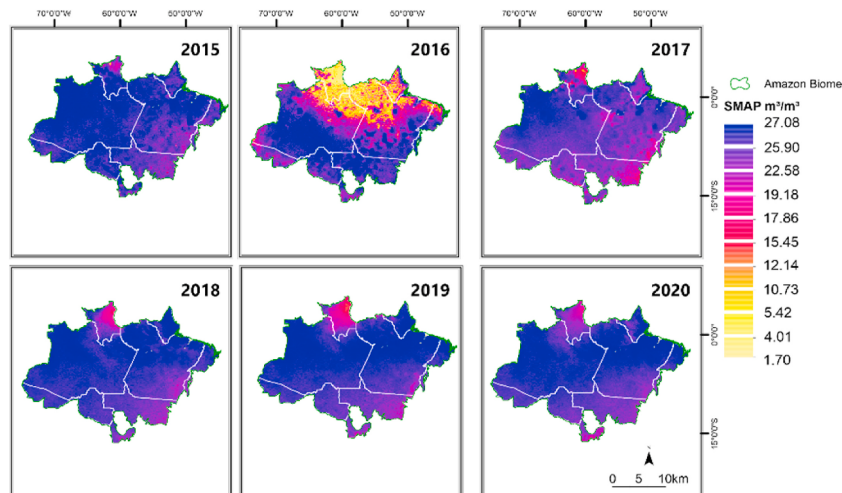


**Fig. 8.** Maps of Soil Moisture Active Passive – SMAP ( $\text{m}^3 \text{ m}^{-3}$ ) from wet period to 2015–2020 in the Amazon biome.

curs with little or no vegetation on the ground. [Andersen et al. \(1998\)](#), bacteria responsible for methane oxidation located on the surface are directly affected by periods of water stress. In addition, in periods of drought, methanogenic bacteria remain protected within the anaerobic interior of soil aggregates, being little or lately impacted by water scarcity ([Andersen et al., 1998; Aceró and González-Asensio, 2018](#)).

For the wet period, no pattern was observed in the distribution of the variable XCH<sub>4</sub>, including 2015 and 2018, and no spatial dependence was shown by the experimental variogram. It is worth noting that in larger observations, XCH<sub>4</sub> tends to be more uniform or homogeneous and consequently reduces the forecast uncertainty. The uncertainty of determining a pattern for the wet season is associated with greater cloudiness for the region of the areas inserted in the Amazon biome, which makes it difficult to observe satellites ([Parazoo et al., 2013](#)).

The results showed that XCH<sub>4</sub> observations can be derived from the Brazilian territory from orbital data to understand the areas inserted in the Amazon biome. However, interesting alternatives in this context use high-resolution atmospheric transport modeling or local terrestrial observation towers, mainly for humid periods, to reduce the uncertainties in the observations ([Feng et al., 2017; Webb et al., 2016](#)).

According to [Wilson et al. \(2020\)](#), the positive trends derived from eastern Amazonia are greater in the wet season, directing an increase in the flow of sources from wetlands as possible drivers of the increase in total methane emissions. However, for the present study, no similar patterns were found that emphasize the same results.

The moderate correlation between Fire Foci and XCH<sub>4</sub> for the wet period suggests biomass burning outside the dry season (June and September). Thus, it corroborates the affirmation of hypothesis "i" of the relationship between fire foci and orbital observations of XCH<sub>4</sub>. In the case of the exceptional droughts in the Amazon of 2015–2016, they are possibly able to explain the relationship between fire foci and XCH<sub>4</sub> ([Marengo et al., 2022](#)).

Taking the Pantanal biome as an example, in the months of January and February during the rainy season, there were unprecedented foci of forest fires ([INPE - Instituto Nacional de Pesquisas Espaciais, 2021](#)). Heavily reported by international media, mostly in late 2019 and 2020 ([Marengo et al., 2021](#)). According to [L. Tunnicliffe et al. \(2020\)](#), climate change tends to be the main driver of emissions for the wet season, mainly due to the rise in surface temperature, thus boosting methane emissions.

Other aspect, the use of Unmanned Aerial Vehicles (UAV) sniffer-based sensor can map changes in the GHGs concentration ([Gålfalk et al., 2021; Mlambo et al., 2017](#)) and perform the wildfire monitoring ([Ivanova et al., 2022; Ausonio et al., 2021](#)). The adoption of UAV remote sensing for XCH<sub>4</sub> and number of fire foci in the Amazon region can be a viable alternative, due to the low temporal and spatial resolution of satellites. Similarly, Machine Learning-Based Approaches for predicting and modeling GHG concentration and wildfire occurrences can be used to all Brazilian biome.

## 5. Conclusions

In the Brazilian Amazon biome, XCH<sub>4</sub> concentrations showed a significant correlation in temporal distribution with SMAP and LST. The spatial distribution of XCH<sub>4</sub> was correlated with the Anomaly XCO<sub>2</sub> but only for the dry period. However, a pattern of spatial distribution XCH<sub>4</sub> was observed for the dry period, consistent with the spatial pattern of SMAP evidenced by the strong positive correlation between XCH<sub>4</sub> and SMAP. This confirmed the hypothesis that XCH<sub>4</sub> shows a positive relationship with SMAP, both for the dry and wet periods under the Amazon biome, and corroborates the positive relationship between the variables. Nonetheless, no pattern was observed in the spatial distribution for XCH<sub>4</sub> concentrations for the wet season, with a moderately positive correlation between XCH<sub>4</sub> and SMAP. This shows that the issue of climate change and land use change significantly interfered in the Amazon ecosystem and can be drivers of

higher CH<sub>4</sub> emissions in the region. Regarding fire foci, there was a moderate correlation between the XCH<sub>4</sub> variable, especially for the wet season. This made it possible to validate hypothesis "i" and helps to foster new scientific studies on GHG emissions for the Amazon biome, especially considering the seasonality of dry and wet periods and the contribution of fire foci.

## Ethical statement

We declare that all ethical practices have been followed in relation to the development, writing, and publication of the article.

## Author statement

Luciano de Souza Maria - Conceptualization, Data curation, Formal analysis, Investigation, Methodology, Project administration, Resources, Software, Supervision, Validation, Writing – original draft. Fernando Saragosa Rossi- Writing – review & editing, Formal analysis, Methodology, Resources, Validation, Visualization, Writing – original draft. Luis Miguel da Costa - Writing – review & editing, Validation, Methodology, Data curation. Marcelo Odorizzi Campos - Writing – review & editing, Data curation, Methodology, Supervision, Validation. Juan Carlos Guerra Blas - Writing – review & editing, Validation, Methodology, Data curation. Alan Rodrigo Panosso - Review & editing, Validation, Software, Methodology, Data curation. Joao Lucas Della Silva - Formal analysis, Methodology, Resources, Validation, Visualization. Carlos Antonio da Silva Junior - Conceptualization, Formal analysis, Investigation, Resources, Supervision, Validation, Writing – review & editing. Newton La Scala Jr - Writing – original draft, Validation, Supervision, Resources, Methodology, Investigation, Formal analysis, Data curation, Conceptualization.

## Declaration of competing interest

The authors declare that they have no known competing financial interests or personal relationships that could have appeared to influence the work reported in this paper.

## Data availability

Data will be made available on request.

## Acknowledgments

The study was funded by Coordenação de Aperfeiçoamento de Pessoal de Nível Superior - Brasil (CAPES). I thank the Geotecnologia Aplicada em Agricultura e Floresta (GAAF) and SojaMaps of the Universidade do Estado de Mato Grosso (UNEMAT) by infrastructure for the present study.

## Appendix A. Supplementary data

Supplementary data to this article can be found online at <https://doi.org/10.1016/j.rsase.2023.100967>.

## References

- Acero, J.A., González-Asensio, B., 2018. Influence of vegetation on the morning land surface temperature in a tropical humid urban area. *Urban Clim.* 26, 231–243. <https://doi.org/10.1016/j.uclim.2018.09.004>.
- Albright, R., Corbett, A., Jiang, X., Creecy, E., Newman, S., Li, K.F., Liang, M.C., Yung, Y.L., 2022. Seasonal variations of solar-induced fluorescence, precipitation, and carbon dioxide over the amazon. *Earth Space Sci.* 9, 1–11. <https://doi.org/10.1029/2021EA002078>.
- Alvares, C.A., Stape, J.L., Sentelhas, P.C., de Moraes Gonçalves, J.L., Sparovek, G., 2013. Köppen's climate classification map for Brazil. *Meteorol. Z.* 22, 711–728. <https://doi.org/10.1127/0941-2948/2013/0507>.
- Andersen, B.L., Bidoglio, G., Leip, A., Rembges, D., 1998. A new method to study simultaneous methane oxidation and methane production in soils. *Global Biogeochem. Cycles* 12, 587–594. <https://doi.org/10.1029/98GB01975>.
- Anderson, L.O., Neto, G.R., Cunha, A.P., Fonseca, M.G., De Moura, Y.M., Dalagnol, R., Wagner, F.H., De Aragão, L.E.O.E.C., 2018. Vulnerability of Amazonian forests to repeated droughts. *Philos. Trans. R. Soc. B Biol. Sci.* 373. <https://doi.org/10.1098/rstb.2017.0411>.
- Antonelli, A., Zizka, A., Carvalho, F.A., Scharn, R., Bacon, C.D., Silvestro, D., Condamine, F.L., 2018. Amazonia is the primary source of Neotropical biodiversity. *Proc. Natl. Acad. Sci. U. S. A* 115, 6034–6039. <https://doi.org/10.1073/pnas.1713819115>.
- Aragão, L.E.O.C., Anderson, L.O., Fonseca, M.G., Rosan, T.M., Vedovato, L.B., Wagner, F.H., Silva, C.V.J., Silva Junior, C.H.L., Arai, E., Aguiar, A.P., Barlow, J., Berenguer, E., Deeter, M.N., Domingues, L.G., Gatti, L., Gloor, M., Malhi, Y., Marengo, J.A., Miller, J.B., Phillips, O.L., Saatchi, S., 2018. 21st Century drought-related fires counteract the decline of Amazon deforestation carbon emissions. *Nat. Commun.* 9, 536. <https://doi.org/10.1038/s41467-017-02771-y>.
- Ausonio, E., Bagnerini, P., Ghio, M., 2021. Drone swarms in fire suppression activities: a conceptual framework. *Drones* 5, 17. <https://doi.org/10.3390/drones5010017>.
- Aybar, C., Wu, Q., Bautista, L., Yali, R., Barja, A., 2020. rgee: an R package for interacting with Google Earth Engine. *J. Open Source Softw.* 5, 2272. <https://doi.org/10.21105/joss.02272>.
- Basso, L.S., Marani, L., Gatti, L.V., Miller, J.B., Gloor, M., Melack, J., Cassol, H.L.G., Tejada, G., Domingues, L.G., Araújo, E., Sanchez, A.H., Corrêa, S.M., Anderson, L., Aragão, L.E.O.C., Correia, C.S.C., Crispim, S.P., Neves, R.A.L., 2021. Amazon methane budget derived from multi-year airborne observations highlights regional variations in emissions. *Commun. Earth Environ.* 2, 1–13. <https://doi.org/10.1038/s43247-021-00314-4>.
- Bousquet, P., Ciais, P., Miller, J.B., Drugokencky, E.J., Hauglustaine, D.A., Prigent, C., Van Der Werf, G.R., Peylin, P., Brunke, E.G., Carouge, C., Langenfelds, R.L., Lathière, J., Papa, F., Ramonet, M., Schmidt, M., Steele, L.P., Tyler, S.C., White, J., 2006. Contribution of anthropogenic and natural sources to atmospheric methane variability. *Nature* 443, 439–443. <https://doi.org/10.1038/nature05132>.
- Brennan, R.W., Phillips, O.L., Feldpausch, T.R., Gloor, E., Baker, T.R., Lloyd, J., Lopez-Gonzalez, G., Monteagudo-Mendoza, A., Malhi, Y., Lewis, S.L., Vásquez Martínez, R., Alexiades, M., Álvarez-Dávila, E., Alvarez-Loayza, P., Andrade, A., Aragão, L.E.O.C., Araujo-Murakami, A., Arets, E.J.M.M., Arroyo, L., Aymard, C., G.A., Bánki, O.S., Baraloto, C., Barroso, J., Bonal, D., Boot, R.G.A., Camargo, J.L.C., Castilho, C.V., Chama, V., Chao, K.J., Chave, J., Comiskey, J.A., Cornejo Valverde, F., Da Costa, L., De Oliveira, E.A., Di Fiore, A., Erwin, T.L., Fauset, S., Forsthofer, M., Galbraith, D.R., Grahame, E.S., Groot, N., Héault, B., Higuchi, N., Honorio Coronado, E.N., Keeling, H., Killeen, T.J., Laurance, W.F., Laurance, S., Licona, J., Magnussen, W.E., Marimon, B.S., Marimon-Junior, B.H., Mendoza, C., Neill, D.A., Nogueira, E.M., Núñez, P., Pallqui Camacho, N.C., Parada, A., Pardo-Molina, G., Peacock, J., Penâ-Claras, M., Pickavance, G.C., Pitman, N.C.A., Poorter, L., Prieto, A., Quesada, C.A., Ramirez, F., Ramirez-Angulo, H., Restrepo, Z., Roopsind, A., Rudas, A., Salomão, R.P., Schwarz, M., Silva, N., Silva-Espejo, J.E., Silveira, M., Stropp, J., Talbot, J., Ter Steege, H., Teran-Aguilar, J., Terborgh, J., Thomas-Caesar, R., Toledo, M., Torello-Raventos, M., Umetsu, R.K., Van Der Heijden, G.M.F., Van Der Hout, P., Guimaraes Vieira, I.C., Vieira, S.A., Vilanova, E., Vos, V.A., Zagt, R.J., 2015. Long-term decline of the Amazon carbon sink. *Nature* 519, 344–348. <https://doi.org/10.1038/nature14283>.
- Cambardella, C.A., Moorman, T.B., Novak, J.M., Parkin, T.B., Karlen, D.L., Turco, R.F., Konopka, A.E., 1994. Field-scale variability of soil properties in central Iowa soils. *Soil Sci. Soc. Am. J.* 58, 1501–1511. <https://doi.org/10.2136/sssaj1994.03615995005800050033x>.
- Carvalho, N.S., Anderson, L.O., Nunes, C.A., Pessôa, A.C.M., Silva Junior, C.H.L., Reis, J.B.C., Shimabukuro, Y.E., Berenguer, E., Barlow, J., Aragão, L.E.O.C., 2021. Spatio-Temporal variation in dry season determines the Amazonian fire calendar. *Environ. Res. Lett.* 16. <https://doi.org/10.1088/1748-9326/ac3aa3>.
- Chevallier, F., Feng, L., Bösch, H., Palmer, P.I., Rayner, P.J., 2010. On the impact of transport model errors for the estimation of CO<sub>2</sub> surface fluxes from GOSAT observations. *Geophys. Res. Lett.* 37. <https://doi.org/10.1029/2010GL044652>.
- Crippa, M., Guizzardi, D., Schaaf, E., Solazzo, E., Muntean, M., Monforti-Ferrario, F., Olivier, J.G.J., Vignati, E., 2021. EDGAR v6.0 greenhouse gas emissions. European Commission, Joint Research Centre (JRC) PID. Retrieved from <http://data.europa.eu/89h/97a67d67-c62e-4826-b873-9d972c4f670b>.
- Crisp, D., Fisher, B.M., O'Dell, C., Frankenberg, C., Basilio, R., Bösch, H., Brown, L.R., Castano, R., Connor, B., Deutscher, N.M., Eldering, A., Griffith, D., Gunson, M., Kuze, A., Mandrake, L., McDuffie, J., Messerschmidt, J., Miller, C.E., Morino, I., Natraj, V., Notholt, J., O'Brien, D.M., Oyafuso, F., Polonsky, I., Robinson, J., Salawitch, R., Sherlock, V., Smyth, M., Suto, H., Taylor, T.E., Thompson, D.R., Wennberg, P.O., Wunch, D., Yung, Y.L., 2012. The ACOS CO<sub>2</sub> retrieval algorithm – Part II: global XCO<sub>2</sub> data characterization. *Atmos. Meas. Technol.* 5, 687–707. <https://doi.org/10.5194/amt-5-687-2012>.
- Crisp, D., Pollock, H.R., Rosenberg, R., Chapsky, L., Lee, R.A.M., Oyafuso, F.A., Frankenberg, C., O'Dell, C.W., Bruegge, C.J., Doran, G.B., Eldering, A., Fisher, B.M., Fu, D., Gunson, M.R., Mandrake, L., Osterman, G.B., Schwandner, F.M., Sun, K., Taylor, T.E., Wennberg, P.O., Wunch, D., 2017. The on-orbit performance of the Orbiting Carbon Observatory-2 (OCO-2) instrument and its radiometrically calibrated products. *Atmos. Meas. Tech.* 10, 59–81. <https://doi.org/10.5194/amt-10-59-2017>.
- Crowell, S., Baker, D., Schuh, A., Basu, S., Jacobson, A.R., Chevallier, F., Liu, J., Deng, F., Feng, L., McKain, K., Chatterjee, A., Miller, J.B., Stephens, B.B., Eldering, A., Crisp, D., Schimel, D., Nassar, R., O'Dell, C.W., Oda, T., Sweeney, C., Palmer, P.I., Jones, D.B.A., 2019. The 2015–2016 carbon cycle as seen from OCO-2 and the global in situ network. *Atmos. Chem. Phys.* 19, 9797–9831. <https://doi.org/10.5194/acp-19-9797-2019>.
- Cui, C., Xu, J., Zeng, J., Chen, K.S., Bai, X., Lu, H., Chen, Q., Zhao, T., 2018. Soil moisture mapping from satellites: an intercomparison of SMAP, SMOS, FY3B, AMSR2, and ESA CCI over two dense network regions at different spatial scales. *Rem. Sens.* 10. <https://doi.org/10.3390/rs10010033>.
- da Costa, L.M., de Araújo Santos, G.A., de Mendonça, et al., 2022a. Spatiotemporal variability of atmospheric CO<sub>2</sub> concentration and controlling factors over sugarcane

- cultivation areas in southern Brazil. Environ. Dev. Sustain. 24, 5694–5717. <https://doi.org/10.1007/s10668-021-01677-6>.
- da Costa, L.M., de Araújo Santos, G.A., Panosso, A.R., et al., 2022b. An empirical model for estimating daily atmospheric column-averaged CO<sub>2</sub> concentration above São Paulo state, Brazil. Carbon Balance Manage. 17, 9. <https://doi.org/10.1186/s13021-022-00209-7>.
- Da Silva Junior, C.A., Lima, M., Teodoro, P.E., de Oliveira-Júnior, J.F., Rossi, F.S., Funatsu, B.M., Butturi, W., Lourençoni, T., Kraeski, A., Pelissari, T.D., Moratelli, F.A., Arvor, D., Luiz, I.M.D.S., Teodoro, L.P.R., Dubreuil, V., Teixeira, V.M., 2022. Fires drive long-term environmental degradation in the amazon basin. Rem. Sens. 14. <https://doi.org/10.3390/rs14020338>.
- Da Silva Junior, C.A., Teodoro, P.E., Delgado, R.C., Teodoro, L.P.R., Lima, M., de Andréa Pantaleão, A., Baio, F.H.R., de Azevedo, G.B., de Oliveira Sousa Azevedo, G.T., Capristo-Silva, G.F., Arvor, D., Facco, C.U., 2020. Persistent fire foci in all biomes undermine the Paris Agreement in Brazil. Sci. Rep. 10, 1–14. <https://doi.org/10.1038/s41598-020-72571-w>.
- Deng, J., 1982. The grey control system. Journal of Huazhong Institute of Technology 10 (3), 9–18.
- Detmers, R.G., Hasekamp, O., Aben, I., Houweling, S., Van Leeuwen, T.T., Butz, A., Landgraf, J., Köhler, P., Guanter, L., Poulter, B., 2015. Anomalous carbon uptake in Australia as seen by GOSAT. Geophys. Res. Lett. 42, 8177–8184. <https://doi.org/10.1002/2015GL065161>.
- Devkota, J.U., 2021. Statistical analysis of active fire remote sensing data: examples from South Asia. Environ. Monit. Assess. 193, 1–14. <https://doi.org/10.1007/s10661-021-09354-x>.
- Entekhabi, D., Njoku, E.G., O'Neill, P.E., Kellogg, K.H., Crow, W.T., Edelstein, W.N., Entin, J.K., Goodman, S.D., Jackson, T.J., Johnson, J., Kimball, J., Piepmeier, J.R., Koster, R.D., Martin, N., McDonald, K.C., Moghaddam, M., Moran, S., Reichle, R., Shi, J.C., Spencer, M.W., Thurman, S.W., Tsang, L., Van Zyl, J., 2010. The soil moisture active passive (SMAP) mission. Proc. IEEE 98, 704–716. <https://doi.org/10.1109/JPROC.2010.2043918>.
- Eufemia, L., Dias Tureta, A.P., Bonatti, M., Da Ponte, E., Sieber, S., 2022. Fires in the amazon region: quick policy review. Dev. Pol. Rev. 1–15. <https://doi.org/10.1111/dpr.12620>.
- Falahatkar, S., Mousavi, S.M., Farajzadeh, M., 2017. Spatial and temporal distribution of carbon dioxide gas using GOSAT data over Iran. Environ. Monit. Assess. 189. <https://doi.org/10.1007/s10661-017-6285-8>.
- Feng, L., Palmer, P.I., Bösch, H., Parker, R.J., Webb, A.J., Correia, C.S.C., Deutscher, N.M., Domingues, L.G., Feist, D.G., Gatti, L.V., Gloor, E., Hase, F., Kivi, R., Liu, Y., Miller, J.B., Morino, I., Sussmann, R., Strong, K., Uchino, O., Wang, J., Zahn, A., 2017. Consistent regional fluxes of CH<sub>4</sub> and CO<sub>2</sub> inferred from GOSAT proxy XCH<sub>4</sub>:CO<sub>2</sub> retrievals, 2010–2014. Atmos. Chem. Phys. 17, 4781–4797. <https://doi.org/10.5194/acp-17-4781-2017>.
- Feng, L., Palmer, P.I., Yang, Y., Yantosca, R.M., Kawa, S.R., Paris, J.-D., Matsueda, H., Machida, T., 2011. Evaluating a 3-D transport model of atmospheric CO<sub>2</sub> using ground-based, aircraft, and space-borne data. Atmos. Chem. Phys. 11, 2789–2803. <https://doi.org/10.5194/acp-11-2789-2011>.
- Frankenberg, C., Pollock, R., Lee, R.A.M., Rosenberg, R., Blavier, J.-F., Crisp, D., O'Dell, C.W., Osterman, G.B., Roehl, C., Wennberg, P.O., Wunch, D., 2015. The Orbiting Carbon Observatory (OCO-2): spectrometer performance evaluation using pre-launch direct sun measurements. Atmos. Meas. Tech. 8, 301–313. <https://doi.org/10.5194/amt-8-301-2015>.
- Gálfalk, M., Nilsson Pälödal, S., Bastviken, D., 2021. Sensitive drone mapping of methane emissions without the need for supplementary ground-based measurements. ACS Earth Space Chem 5, 2668–2676. <https://doi.org/10.1021/acsearthspacechem.1c00106>.
- Giglio, L., Descloux, J., Justice, C.O., Kaufman, Y.J., 2003. An enhanced contextual fire detection algorithm for MODIS. Remote Sens. Environ. 87, 273–282. [https://doi.org/10.1016/S0034-4257\(03\)00184-6](https://doi.org/10.1016/S0034-4257(03)00184-6).
- Guerlet, S., Basu, S., Butz, A., Krol, M., Hahne, P., Houweling, S., Hasekamp, O.P., Aben, I., 2013. Reduced carbon uptake during the 2010 Northern Hemisphere summer from GOSAT. Geophys. Res. Lett. 40, 2378–2383. <https://doi.org/10.1002/grl.50402>.
- Guo, M., Li, J., Wen, L., Huang, S., 2019. Estimation of CO<sub>2</sub> emissions from Wildfires using OCO-2 data. Atmosphere 10, 1–16. <https://doi.org/10.3390/atmos10100581>.
- Guo, M., Li, J., Xu, J., Wang, X., He, H., Wu, L., 2017. CO<sub>2</sub> emissions from the 2010 Russian wildfires using GOSAT data. Environ. Pollut. 226, 60–68. <https://doi.org/10.1016/j.envpol.2017.04.014>.
- Hakkarainen, J., Ialongo, I., Tamminen, J., 2016. Direct space-based observations of anthropogenic CO<sub>2</sub> emission areas from OCO-2. Geophys. Res. Lett. 43 (11). <https://doi.org/10.1002/2016GL070885>. 400-11,406.
- Heinrich, V.H.A., Dalagnol, R., Cassol, H.L.G., Rosan, T.M., de Almeida, C.T., Silva Junior, C.H.L., Campanharo, W.A., House, J.I., Sitch, S., Hales, T.C., Adami, M., Anderson, L.O., Aragão, L.E.O.C., 2021. Large carbon sink potential of secondary forests in the Brazilian Amazon to mitigate climate change. Nat. Commun. 12, 1–11. <https://doi.org/10.1038/s41467-021-22050-1>.
- Heymann, J., Reuter, M., Buchwitz, M., Schneising, O., Bovensmann, H., Burrows, J.P., Massart, S., Kaiser, J.W., Crisp, D., 2017. CO<sub>2</sub> emission of Indonesian fires in 2015 estimated from satellite-derived atmospheric CO<sub>2</sub> concentrations. Geophys. Res. Lett. 44, 1537–1544. <https://doi.org/10.1002/2016GL072042>.
- Hyoungh, J.L., 2021. Prediction of large-scale wildfires with the canopy stress index derived from soil moisture active passive. IEEE J. Sel. Top. Appl. Earth Obs. Rem. Sens. 14, 2096–2102. <https://doi.org/10.1109/JSTARS.2020.3048067>.
- Instituto Brasileiro de Geografia e Estatística (Brazilian Institute of Geography and Statistics)-IBGE, 2020. Conheça cidades e Estados do Brasil. São Paulo, Brazil.
- INPE - Instituto Nacional de Pesquisas Espaciais, 2021. Portal Do Monitoramento de Queimadas e Incêndios (Brazilian National Institute for Space Research - wildfires monitoring program). <http://www.inpe.br/queimadas>.
- Intergovernmental Panel on Climate Change - IPCC, 2022. Summary for policymakers. H.-O. Pörtner, D.C. Roberts, E.S. Poloczanska, K. Mintenbeck, M. Tignor, A. Alegria, M. Craig, S. Langsdorf, S. Löschke, V. Möller, A. Okem (eds.). In: Pörtner, H.-O., Roberts, D.C., Tignor, M., Poloczanska, E.S., Mintenbeck, K., Alegria, M., Craig, M., Langsdorf, S., Löschke, S., Möller, V., Okem, A., Rama, B. (Eds.), Climate Change 2022: Impacts, Adaptation and Vulnerability. Contribution of Working Group II to the Sixth Assessment Report of the Intergovernmental Panel on Climate Change. Cambridge University Press, Cambridge, UK and New York, NY, USA, pp. 3–33. <https://doi.org/10.1017/9781009325844.001>.
- Isaaks, E.H., Srivastava, R.M., 1989. An Introduction to Applied Geostatistics, first ed. Oxford University Press, Oxford, p. 561.
- Ivanova, S., Prosekov, A., Kaledin, A., 2022. A survey on monitoring of wild animals during fires using drones. Fire 5, 60. <https://doi.org/10.3390/fire5030060>.
- Jiang, X., Li, K.F., Liang, M.C., Yung, Y.L., 2021. Impact of amazonian fires on atmospheric CO<sub>2</sub>. Geophys. Res. Lett. 48, 1–10. <https://doi.org/10.1029/2020GL091875>.
- Kirschke, S., Bousquet, P., Ciais, P., Saunois, M., Canadell, J.G., Slugokenky, E.J., Bergamaschi, P., Bergmann, D., Blake, D.R., Bruhwiler, L., Cameron-Smith, P., Castaldi, S., Chevallier, F., Feng, L., Fraser, A., Heimann, M., Hodson, E.L., Houweling, S., Josse, B., Fraser, P.J., Krummel, P.B., Lamarque, J.F., Langenfelds, R.L., Le Quéré, C., Naik, V., O'Doherty, S., Palmer, P.I., Pison, I., Plummer, D., Poulter, B., Prinn, R.G., Rigby, M., Ringeval, B., Santini, M., Schmidt, M., Shindell, D.T., Simpson, I.J., Spahni, R., Steele, L.P., Strode, S.A., Sudo, K., Szopa, S., Van Der Werf, G.R., Voulgarakis, A., Van Weele, M., Weiss, R.F., Williams, J.E., Zeng, G., 2013. Three decades of global methane sources and sinks. Nat. Geosci. 6, 813–823. <https://doi.org/10.1038/ngeo1955>.
- Le Roux, R., Wagner, F., Blanc, L., Betbeder, J., Gond, V., Dessard, H., Funatsu, B., Bourgois, C., Cornu, G., Herault, B., Montfort, F., Sist, P., Begue, A., Dubreuil, V., Laurent, F., Messner, F., Fadhl Hasan, A., Arvor, D., 2022. How wildfires increase sensitivity of Amazon forests to droughts. Environ. Res. Lett. 17, 044031. <https://doi.org/10.1088/1748-9326/ac5b3d>.
- Li, L., Lei, L., Song, H., Zeng, Z., He, Z., 2022. Spatiotemporal geostatistical analysis and global mapping of CH<sub>4</sub> columns from GOSAT observations. Rem. Sens. 14. <https://doi.org/10.3390/rs14030654>.
- Marengo, J.A., Cunha, A.P., Cuartas, L.A., Deusdará Leal, K.R., Broedel, E., Seluchi, M.E., Michelin, C.M., De Praga Baião, C.F., Chuchón Ángulo, E., Almeida, E.K., Kazmierczak, M.L., Mateus, N.P.A., Silva, R.C., Bender, F., 2021. Extreme drought in the Brazilian pantanal in 2019–2020: characterization, causes, and impacts. Front. Water 3. <https://doi.org/10.3389/frwa.2021.639204>.
- Marengo, J.A., Jimenez, J.C., Espinoza, J.C., Cunha, A.P., Aragão, L.E.O., 2022. Increased climate pressure on the agricultural frontier in the Eastern Amazonia–Cerrado transition zone. Sci. Rep. 12, 1–10. <https://doi.org/10.1038/s41598-021-04241-4>.
- Marengo, J.A., Souza, C.M., Thonicke, K., Burton, C., Halladay, K., Betts, R.A., Alves, L.M., Soares, W.R., 2018. Changes in climate and land use over the amazon region: current and future variability and trends. Front. Earth Sci. 6, 1–21. <https://doi.org/10.3389/feart.2018.00228>.
- Mlambo, R., Woodhouse, I.H., Gerard, F., Anderson, K., 2017. Structure from motion (SfM) photogrammetry with drone data: a low cost method for monitoring greenhouse gas emissions from forests in developing countries. Forests 8, 68. <https://doi.org/10.3390/f8030068>.
- Morgan, W.T., Derbyshire, E., Spracklen, D.V., Artaxo, P., Coe, H., 2019. Non-deforestation drivers of fires are increasingly important sources of aerosol and carbon

- dioxide emissions across Amazonia. *Sci. Rep.* 9, 1–15. <https://doi.org/10.1038/s41598-019-53112-6>.
- Nikitenko, A.A., Timofeev, Y.M., Berezin, I.A., Poberovskii, A.V., Virolainen, Y.A., Polyakov, A.V., 2020. The analysis of OCO-2 satellite measurements of CO<sub>2</sub> in the vicinity of Russian cities. *Atmos. Ocean. Opt.* 33, 650–655. <https://doi.org/10.1134/S1024856020060111>.
- Nisbet, E.G., Manning, M.R., Dlugokencky, E.J., Fisher, R.E., Lowry, D., Michel, S.E., Myhre, C.L., Platt, S.M., Allen, G., Bousquet, P., Brownlow, R., Cain, M., France, J.L., Hermansen, O., Hossaini, R., Jones, A.E., Levin, I., Manning, A.C., Myhre, G., Pyle, J.A., Vaughn, B.H., Warwick, N.J., White, J.W.C., 2019. Very strong atmospheric methane growth in the 4 Years 2014–2017: implications for the paris agreement. *Global Biogeochem. Cycles* 33, 318–342. <https://doi.org/10.1029/2018GB006009>.
- Nobre, C.A., Sampaio, G., Borma, L.S., Castilla-Rubio, J.C., Silva, J.S., Cardoso, M., 2016. Land-use and climate change risks in the amazon and the need of a novel sustainable development paradigm. *Proc. Natl. Acad. Sci. U. S. A* 113, 10759–10768. <https://doi.org/10.1073/pnas.1605516113>.
- O'Dell, C.W., Connor, B., Bösch, H., O'Brien, D., Frankenberg, C., Castano, R., Christi, M., Eldering, D., Fisher, B., Gunson, M., McDuffie, J., Miller, C.E., Natraj, V., Oyafuso, F., Polonsky, I., Smyth, M., Taylor, T., Toon, G.C., Wennberg, P.O., Wunch, D., 2012. The ACOS CO&lt;sub&gt;2&lt;/sub&gt; retrieval algorithm – Part 1: description and validation against synthetic observations. *Atmos. Meas. Tech.* 5, 99–121. <https://doi.org/10.5194/amt-5-99-2012>.
- Oguma, H., Morino, I., Suto, H., Yoshida, Y., Eguchi, N., Kuze, A., Yokota, T., 2011. First observations of CO<sub>2</sub> absorption spectra recorded in 2005 using an airship-borne FTS (GOSAT TANSO-FTS BBM) in the SWIR spectral region. *Int. J. Rem. Sens.* 32, 9033–9049. <https://doi.org/10.1080/01431161.2010.535864>.
- Parazoo, N.C., Bowman, K., Frankenberg, C., Lee, J.-E., Fisher, J.B., Worden, J., Jones, D.B.A., Berry, J., Collatz, G.J., Baker, I.T., Jung, M., Liu, J., Osterman, G., O'Dell, C., Sparks, A., Butz, A., Guerlet, S., Yoshida, Y., Chen, H., Gerbig, C., 2013. Interpreting seasonal changes in the carbon balance of southern Amazonia using measurements of XCO<sub>2</sub> and chlorophyll fluorescence from GOSAT. *Geophys. Res. Lett.* 40, 2829–2833. <https://doi.org/10.1002/grl.50452>.
- Parker, R., Boesch, H., Cogan, A., Fraser, A., Feng, L., Palmer, P.I., Messerschmidt, J., Deutscher, N., Griffith, D.W.T., Notholt, J., Wennberg, P.O., Wunch, D., 2011. Methane observations from the Greenhouse Gases Observing SATellite: comparison to ground-based TCCON data and model calculations. *Geophys. Res. Lett.* 38, <https://doi.org/10.1029/2011GL047871>.
- Parker, R.J., Boesch, H., Byckling, K., Webb, A.J., Palmer, P.I., Feng, L., Bergamaschi, P., Chevallier, F., Notholt, J., Deutscher, N., Warneke, T., Hase, F., Sussmann, R., Kawakami, S., Kivi, R., Griffith, D.W.T., Velasco, V., 2015. Assessing 5 years of GOSAT Proxy XCH&lt;sub&gt;2&lt;/sub&gt; data and associated uncertainties. *Atmos. Meas. Tech.* 8, 4785–4801. <https://doi.org/10.5194/amt-8-4785-2015>.
- Peters, W., Jacobson, A.R., Sweeney, C., Andrews, A.E., Conway, T.J., Masarie, K., Miller, J.B., Bruhwiler, L.M.P., Pétron, G., Hirsch, A.I., Worthy, D.E.J., van der Werf, G.R., Randerson, J.T., Wennberg, P.O., Krol, M.C., Tans, P.P., 2007. An atmospheric perspective on North American carbon dioxide eXCHange: CarbonTracker. *Proc. Natl. Acad. Sci. USA* 104, 18925–18930. <https://doi.org/10.1073/pnas.0708986104>.
- Pontes-Lopes, A., Silva, C.V.J., Barlow, J., Rincón, L.M., Campanharo, W.A., Nunes, C.A., De Almeida, C.T., Silva Júnior, C.H.L., Cassol, H.L.G., Dalagnol, R., Stark, S.C., Graça, P.M.L.A., Aragão, L.E.O.C., 2021. Drought-driven wildfire impacts on structure and dynamics in a wet Central Amazonian forest. *Proc. R. Soc. B Biol. Sci.* 288. <https://doi.org/10.1098/rspb.2021.0094>.
- Ross, A.N., Wooster, M.J., Boesch, H., Parker, R., 2013. First satellite measurements of carbon dioxide and methane emission ratios in wildfire plumes. *Geophys. Res. Lett.* 40, 4098–4102. <https://doi.org/10.1002/grl.50733>.
- Rossi, F.S., Araújo Santos, G.A., Maria, L.S., Lourençoni, T., Pelissari, T.D., Della-Silva, J.L., Oliveira Júnior, Silva, A.A., Lima, M., Teodoro, P.E., Teodoro, L.P.E., Oliveira-Júnior, J.F., La Scala, Jr., N., Silva Junior, C.A., 2022. Carbon dioxide spatial variability and dynamics for contrasting land uses in central Brazil agricultural frontier from remote sensing data. *J. South Am. Earth Sci.* 116, 103809. <https://doi.org/10.1016/j.jsames.2022.103809>.
- Saatchi, S., Longo, M., Xu, L., Yang, Y., Abe, H., André, M., Aukema, J.E., Carvalhais, N., Cadillo-Quiroz, H., Cerbu, G.A., Cherney, J.M., Covey, K., Sánchez-Clavijo, L.M., Cubillos, I.V., Davies, S.J., De Sy, V., De Vleeschouwer, F., Duque, A., Sybille Durieux, A.M., De Avila Fernandes, K., Fernandez, L.E., Gammino, V., Garrity, D.P., Gibbs, D.A., Gibbon, L., Gowae, G.Y., Hansen, M., Lee Harris, N., Healey, S.P., Hilton, R.G., Johnson, C.M., Kankeur, R.S., Laporte-Goetz, N.T., Lee, H., Lovejoy, T., Lowman, M., Lumbuenamo, R., Malhi, Y., Albert Martinez, J.M.M., Nobre, C., Pellegrini, A., Radachowsky, J., Román, F., Russell, D., Sheil, D., Smith, T.B., Spencer, R.G.M., Stolle, F., Tata, H.L., Torres, D. del C., Tshimanga, R.M., Vargas, R., Venter, M., West, J., Widayati, A., Wilson, S.N., Brumby, S., Elmore, A.C., 2021. Detecting vulnerability of humid tropical forests to multiple stressors. *One Earth* 4, 988–1003. <https://doi.org/10.1016/j.oneear.2021.06.002>.
- Saunois, M., Stavert, R., Poulter, B., Bousquet, P., Canadell, G., Jackson, B., Raymond, R.A., J. P., Dlugokencky, E., Houweling, S., Patra, K., Ciais, P., Arora, K., Bastviken, D., Bergamaschi, P., Blake, R., Brailsford, G., Bruhwiler, L., Carlson, M., Carroll, M., Castaldi, S., Chandra, N., Crevoisier, C., Crill, M., Covey, K., Curry, L., Etiope, G., Frankenberg, C., Gedney, N., Hegglin, I., Höglund-Isaksson, L., Hugelius, G., Ishizawa, M., Ito, A., Janssens-Maenhout, G., Jensen, M., Joos, F., Kleinen, T., Krummel, B., Langenfelds, P.L., Laruelle, G., Liu, L., MacHida, T., Maksyutov, S., McDonald, C., McNorton, J., Miller, A., Melton, P.R., Morino, I., Müller, J., Murguia-Flores, F., Naik, V., Niwa, Y., Noce, S., O'Doherty, S., Parker, J., Peng, C., Peng, S., Peters, P., Prigent, C., Prinn, R., Ramonet, M., Regnier, P., Riley, J., Rosentreter, W.A., Segers, A., Simpson, I., Shi, H., Smith, J., Paul Steele, L., Thornton, F., Tian, H., Tohjima, Y., Tubiello, N., Tsuruta, A., Viovy, N., Voulgarakis, A., Weber, S., Van Weele, T., Van Der Werf, M.R., Weiss, G.F., Worthy, D., Wunch, D., Yin, Y., Yoshida, Y., Zhang, W., Zhang, Z., Zhao, Y., Zheng, B., Zhu, Qing, Zhu, Qiuhan, Zhuang, Q., 2020. The global methane budget 2000–2017. *Earth Syst. Sci. Data* 12, 1561–1623. <https://doi.org/10.5194/essd-12-1561-2020>.
- Silva, C.H.L., Aragão, L.E.O.C., Fonseca, M.G., Almeida, C.T., Vedovato, L.B., Anderson, L.O., 2018. Deforestation-induced fragmentation increases forest fire occurrence in central Brazilian Amazonia. *Forests* 9. <https://doi.org/10.3390/f9060305>.
- Teodoro, P.E., da Silva Junior, C.A., Delgado, R.C., Lima, M., Teodoro, L.P.R., Baio, F.H.R., de Oliveira Sousa Azevedo, G.T., de Andréa Pantaleão, A., Capristo-Silva, G.F., Facco, C.U., 2022. Twenty-year impact of fire foci and its relationship with climate variables in Brazilian regions. *Environ. Monit. Assess.* 194. <https://doi.org/10.1007/s10661-021-09702-x>.
- Trangmar, B.B., Yost, R.S., Uehara, G., 1986. Application of geostatistics to spatial studies of soil properties. In: Brady, N.C. (Ed.), *Advances in Agronomy*. Academic Press, pp. 45–94. [https://doi.org/10.1016/S0065-2113\(08\)60673-2](https://doi.org/10.1016/S0065-2113(08)60673-2).
- Tunncliffe, R.L., Ganeshan, A.L., Parker, R.J., Boesch, H., Gedney, N., Poulter, B., Zhang, Z., Lavrič, J.V., Walter, D., Rigby, M., Henne, S., Young, D., O'Doherty, S., 2020. Quantifying sources of Brazil's ch<sub>4</sub> emissions between 2010 and 2018 from satellite data. *Atmos. Chem. Phys.* 20, 13041–13067. <https://doi.org/10.5194/acp-20-13041-2020>.
- Wan, Z., 2008. New refinements and validation of the MODIS Land-Surface Temperature/Emissivity products. *Remote Sens. Environ.* 112, 59–74. <https://doi.org/10.1016/j.rse.2006.06.026>.
- Webb, A.J., Bösch, H., Parker, R.J., Gatti, L.V., Gloo, E., Palmer, P.I., Basso, L.S., Chipperfield, M.P., Correia, C.S.C., Domingues, L.G., Feng, L., Gonzi, S., Miller, J.B., Warneke, T., Wilson, C., 2016. CH<sub>4</sub> concentrations over the Amazon from GOSAT consistent with in situ vertical profile data. *J. Geophys. Res.* 121 (11). <https://doi.org/10.1002/2016JD025263>. 006-11,020.
- Webster, R., Oliver, M.A., 1990. *Statistical Methods in Soil and Land Resource Survey*, first ed. Oxford University Press (OUP), Oxford.
- Wecht, K.J., Jacob, D.J., Sulprizio, M.P., Santoni, G.W., Wofsy, S.C., Parker, R., Bösch, H., Worden, J., 2014. Spatially resolving methane emissions in California: constraints from the CalNex aircraft campaign and from present (GOSAT, TES) and future (TROPOMI, geostationary) satellite observations. *Atmos. Chem. Phys.* 14, 8173–8184. <https://doi.org/10.5194/acp-14-8173-2014>.
- Wilson, C., Chipperfield, M.P., Gloo, M., Parker, R.J., Boesch, H., McNorton, J., Gatti, L.V., Miller, J.B., Basso, L.S., Monks, S.A., 2020. Large and increasing methane emissions from Eastern Amazonia derived from satellite data, 2010–2018. *Atmos. Chem. Phys. Discuss.* 2020, 1–38. <https://doi.org/10.5194/acp-2020-1136>.
- Yin, S., Wang, X., Tani, H., Zhang, X., Zhong, G., Sun, Z., Chittenden, A.R., 2018. Analyzing temporo-spatial changes and the distribution of the CO<sub>2</sub> concentration in Australia from 2009 to 2016 by greenhouse gas monitoring satellites. *Atmos. Environ.* 192, 1–12. <https://doi.org/10.1016/j.atmosenv.2018.08.043>.
- Zemp, D.C., Schlieussner, C.-F., Barbosa, H.M.J., Hirota, M., Montade, V., Sampaio, G., Staal, A., Wang-Erlundsson, L., Rammig, A., 2017. Self-amplified Amazon forest loss due to vegetation-atmosphere feedbacks. *Nat. Commun.* 8, 14681. <https://doi.org/10.1038/ncomms14681>.